

## Full Length Article

# Genome-wide DNA methylation profiling of hip articular cartilage identifies differentially methylated loci associated with osteonecrosis of the femoral head



Junlong Wu<sup>a,c,1</sup>, Yanan Du<sup>b,1</sup>, Jidong Song<sup>a</sup>, Xiaoqian Dang<sup>a</sup>, Kunzheng Wang<sup>a</sup>, Yan Wen<sup>b</sup>, Feng Zhang<sup>b,\*</sup>, Ruiyu Liu<sup>a,\*\*</sup>

<sup>a</sup> Department of Orthopedics, the Second Affiliated Hospital, Xi'an Jiaotong University, Xi'an, PR China

<sup>b</sup> Key Laboratory of Trace Elements and Endemic Diseases, Collaborative Innovation Center of Endemic Disease and Health Promotion for Silk Road Region, School of Public Health, Health Science Center, Xi'an Jiaotong University, Xi'an, PR China

<sup>c</sup> Luoyang Central Hospital Affiliated to Zhengzhou University, Luoyang, Henan Province, 471009, China

## ARTICLE INFO

## Keywords:

Osteonecrosis of the femoral head  
Genome-wide DNA methylation  
Hip articular cartilage  
Pathway enrichment analysis

## ABSTRACT

**Objective:** Recent studies demonstrated a critical role of hip articular cartilage destruction in the development of osteonecrosis of the femoral head (ONFH). The aim of this study was to characterize the genome-wide DNA methylation profile of hip cartilage obtained from patients with ONFH and healthy subjects.

**Methods:** Hip articular cartilage specimens were collected from 15 ONFH patients (including 11 males and 4 females) and 15 control subjects (including 11 males and 4 females) with femoral neck fracture. The average ages of the ONFH patients and control subjects were  $50.27 \pm 5.27$  years and  $61.67 \pm 3.38$  years, respectively. Genome-wide DNA methylation profiles of 5 ONFH and 5 control cartilages were determined by Illumina HumanMethylation850 array. Differential methylation analysis of DNA methylation profiles were performed by the empirical Bayes moderated *t*-test of the limma package. Mass spectrograph (MS) analysis of 10 ONFH cartilages and 10 normal cartilages were performed to validate the results of genome-wide DNA methylation profiling. Immunohistochemistry (IHC) of 4 ONFH cartilages and 4 control cartilages were conducted to evaluate the expression levels of proteins encoded by identified differentially methylated genes. *t*-test was used to assess the significance of protein expression differences between ONFH patients and controls in IHC.

**Results:** We identified a total of 2872 differentially methylated CpG sites, annotated to 480 hypermethylated genes and 1335 hypomethylated genes for ONFH. The results of MS validation were consistent with that of genome-wide DNA methylation profiling. IHC further confirmed the increased protein expression of CARS (mean and 95%CI of superficial zone 59.67% [48.46, 56.14], and deep zone 31% [25.85, 30.61]), PDE4D (superficial zone 50.33% [33.64, 40.68] and deep zone 28.67% [10.81, 36.47]), ADAMTS12 (superficial zone 53.67% [36.01, 40.93] and deep zone 34.67% [22.56, 37.18]), LRP5 (superficial zone 59.63% [27.32, 39.61] and deep zone 22.95% [5.28, 19.29]), RUNX2 (superficial zone 52.58% [11.64, 31.33] and deep zone 35.01% [10.03, 27.44]) in ONFH articular cartilage.

**Conclusion:** Our results suggest the implication of DNA methylation alterations in the development of ONFH, and provide novel clues for pathogenetic and therapeutic studies of ONFH.

## 1. Introduction

Osteonecrosis of the femoral head (ONFH) is a seriously disabling disease, usually affecting young adults aged between 35 and 55 [1].

There are about 8.12 million patients with non-traumatic ONFH in China now [2]. It was reported that 2.0–3.0 million cases were diagnosed with ONFH every year in the United States [3]. ONFH can be caused by traumatic events and non-traumatic conditions, such as

\* Correspondences to: F. Zhang, School of Public Health, Health Science Center, Xi'an Jiaotong University, No. 76 Yan Ta West Road, Xi'an 710061, China.

\*\* Correspondence to: R. Liu, Department of Orthopedics, the Second Affiliated Hospital, Health Science Center, Xi'an Jiaotong University, No. 76 Yan Ta West Road, Xi'an 710061, China.

E-mail addresses: [fzhxjtu@mail.xjtu.edu.cn](mailto:fzhxjtu@mail.xjtu.edu.cn) (F. Zhang), [liuryu@126.com](mailto:liuryu@126.com) (R. Liu).

<sup>1</sup> These two authors contribute equally to this manuscript.

<https://doi.org/10.1016/j.bone.2019.06.021>

Received 10 October 2018; Received in revised form 9 June 2019; Accepted 20 June 2019

Available online 21 June 2019

8756-3282/ © 2019 Elsevier Inc. All rights reserved.

alcoholism, corticosteroid therapy and hematologic disease [4]. In the early stage of ONFH, hip pain is the main clinical symptom. With the development of ONFH, it leads to rapid destruction and dysfunction of hip joint [5]. Because the pathogenesis of ONFH remains elusive, there is not recognized effective treatment for ONFH now. About 65% ONFH patients finally need total hip replacement [6], resulting in heavy medical and economic burden to the patients.

ONFH is pathologically characterized by the death of osteocytes and bone marrow cells due to inadequate blood supply of subchondral bone [1]. During the reparative process of necrotic bone, the imbalance between bone resorption and bone reformation results in the structural damage and collapse of the femoral head. Although the destruction of hip articular cartilage is not the initial damage of ONFH, recent studies demonstrated a critical role of hip articular cartilage in the development of ONFH and articular cartilage degeneration occurs at the early-stage of ONFH [7]. For instance, damaged hip articular cartilage is capable of increasing the instability of hip, exacerbating the collapse of the femoral head and accelerating the development of ONFH [8]. Treatment of articular cartilage degeneration should be benefit for ONFH patients before femoral head collapse or early stage of femoral head collapse. Therefore, early treatment of hip articular cartilage damage may help to slow the hip destruction of ONFH and prolong time to surgery. However, limited efforts were paid to explore the mechanism of hip articular cartilage destruction in ONFH. The biological mechanism of hip articular cartilage destruction remains unclear now.

It has been demonstrated that genetic factors contributed greatly to the development of ONFH [9]. Several susceptibility genes have been identified for ONFH, such as *COL2A1* [10], *MTHFR* [11] and *PON1* [12]. However, the genetic risk of ONFH explained by the identified loci was limited, suggesting the existence of undiscovered genetic factors for ONFH. DNA methylation, one of primary epigenetic mechanism, is responsible for gene expression regulation by silencing transposable elements and altering the transcriptional accessibility of regulatory genomic regions [13]. CpG sites are the DNA regions where a cytosine nucleotide and a guanine nucleotide was separated by one phosphate group, that is, 5'-C—phosphate—G—3'. DNA methylation can occur at the 5 position of the pyrimidine ring of the cytosine residues within the CpG sites to form 5-methylcytosines. The methylation of CpG sites of promoters can silence the expression of target genes. Recently, multiple studies confirmed the implication of abnormal DNA methylation in the pathogenesis of bone and cartilage diseases [14,15]. Primary osteoarthritis (OA) is a chronic degenerative joint disease characterized by degradation of articular cartilage. Multiple genome-wide DNA methylation profiling of OA articular cartilage have been conducted [14]. However, because the etiology and pathologic features of articular cartilage lesions between OA and ONFH are different, methylation study results of OA may provide limited information for the pathogenetic studies of the cartilage degeneration of ONFH. No genome-wide DNA methylation profiling of ONFH hip articular cartilage has been conducted by now. The potential roles of DNA methylation in the hip articular cartilage destruction of ONFH are largely unknown.

In this study, using the Illumina Infinium HumanMethylation 850 BeadChip, we conducted a genome-wide DNA methylation profiling of hip articular cartilage from ONFH patients and healthy control subjects. We identified a group of significantly differentially methylated genes. The functional relevance of the identified genes with ONFH was further validated by mass spectrograph analysis (MS) and immunohistochemistry (IHC) using two independent validation samples. Our results demonstrated the implication of altered DNA methylation in the hip articular cartilage damage of ONFH, and identified multiple candidate genes and biological pathways for subsequent functional studies of ONFH.

**Table 1**  
Basic characteristics of the study subjects.

Group	ONFH		Normal	
	Age (years)	Gender	Age (years)	Gender
Methylation chip				
1	50	Female	61	Female
2	54	Male	60	Male
3	52	Male	63	Male
4	51	Male	61	Male
5	55	Male	65	Male
Mass spectrograph				
6	48	Male	59	Male
7	45	Male	62	Male
8	53	Male	60	Male
9	50	Male	65	Male
10	56	Female	62	Female
11	43	Female	63	Female
Mass spectrograph and immunohistochemistry				
12	36		54	Male
13	54	Male	57	Male
14	56	Male	65	Male
15	51	Female	68	Female

Note: ONFH, osteonecrosis of the femoral head.

## 2. Materials and methods

A genome-wide DNA methylation profiling was first conducted to scan differentially methylated genes between ONFH cartilage and control cartilage specimens. The top two of differentially methylated genes were selected for further MS validation. IHC was finally conducted to compare the proteins expression levels of identified candidate genes between ONFH cartilage and control cartilage specimens.

### 2.1. Cartilage specimen collection

Human subjects were recruited from the Second Affiliated Hospital of Xi'an Jiaotong University. Totally, 30 hip articular cartilage specimens were used in this study (Table 1). All study subjects were Chinese Han undergoing total hip replacement surgery. ONFH patients and control subjects were diagnosed according to clinical manifestations and radiologic imaging of the hip by two blinded ONFH experts. ONFH hip articular cartilage specimens were obtained from 15 grade III idiopathic-ONFH patients classified by the Ficat system [16]. Grade III articular cartilage specimens were natural models with subchondral osteonecrosis, nutritional deficiency and cartilage degeneration. Normal hip articular cartilage specimens were collected from 15 subjects having femoral neck fracture and undergoing total hip replacement. Clinical data for each study subject was collected by nurse-administered questionnaire, including self-reported ethnicity, lifestyle characteristics, health status, and family and medical history. The subjects with osteoarthritis (OA), rheumatoid arthritis (RA), or other hip disorders were excluded. Hip articular cartilage specimens were collected from the same anatomic areas of antero-superior portions of the femoral head, where the articular cartilage collapsed (Fig. 1). Five, ten, and four ONFH-control pairs were used for genome-wide DNA methylation profiling, MS and IHC experiments, respectively. This study was approved by the Human Ethics Committees of Xi'an Jiaotong University. Inform-consent documents were signed by all participants before participating this study.

### 2.2. DNA extraction

For genome-wide DNA methylation profiling and MS validation analysis, cartilage specimens were dissected and rapidly frozen in liquid nitrogen. DNA was then isolated from the cartilage specimens using QIAamp DNA Mini Kit (QIAGEN, Germany) following the

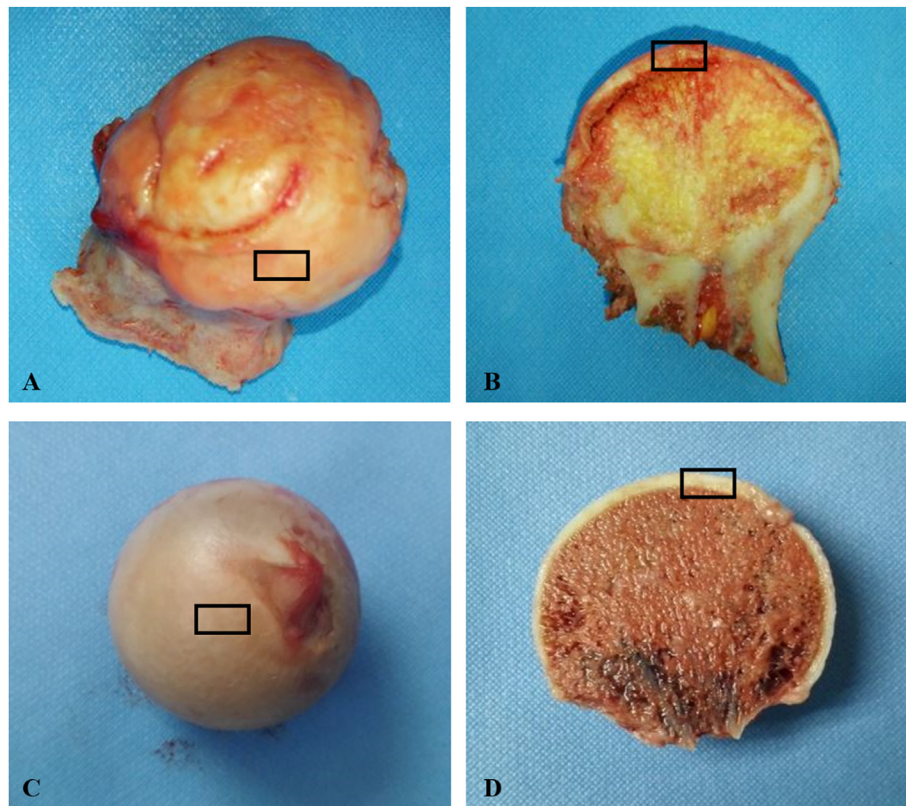


Fig. 1. Images of femoral heads from ONFH patients (A and B) and healthy controls (C and D).

manufacturer's recommended protocol. The concentration (50 ng/ $\mu$ L, 20  $\mu$ L) of isolated total DNA was determined by NanoDrop ND-2000 Spectrophotometer (Thermo Fisher Scientific Inc., USA). The quality of extracted DNA was evaluated with 0.8% agarose gel electrophoresis.

### 2.3. Genome-wide DNA methylation profiling

Genome-wide DNA methylation profiling of hip articular cartilage specimens from 5 ONFH patients and 5 healthy controls, was conducted using the Illumina Infinium HumanMethylation 850 BeadChip according to the manufacturer's standard procedure. In brief, EZ DNA Methylation Kit (Zymo Research, USA) was used to perform bisulfite treatment of 500 ng DNA samples. The bisulfite converted DNA were then amplified, hybridized to HumanMethylation850 array, stained and washed following standard protocol. Raw image intensities were scanned by iScan SQ scanner (iScan System, Illumina, USA) and processed by Genome Studio software (Illumina, USA). The lumi (version 2.22.1) [17] and BMIQ (version 1.3) [18] packages of R were used to normalize the raw image intensity data. The percentage of methylated cytosine at a given CpG site was calculated as a  $\beta$  value, varying from 0.0 (completely unmethylated) to 1.0 (completely methylated). Generalized linear mixed model was used to adjust age and sex as covariates. We exclude the CpG probes mapping to sex chromosomes, crossly reacting with sex chromosomes or containing genetic variants. A total of 844,832 CpG sites passing quality control procedure were analyzed in this study. The Pearson correlation coefficients of  $\beta$  values were calculated to evaluate the correlations of samples.

### 2.4. Differential methylation analysis

Differentially methylated CpG sites were identified by the empirical Bayes moderated *t*-test of the limma package (version 3.1.2, <https://bioconductor.org/packages/release/bioc/html/limma.html>) of R [19] using DNA methylation M-values. The Benjamini–Hochberg method

was used to obtain an adjusted *P* value for each CpG locus. The CpG sites with adjusted *P* value  $\leq 0.05$  and  $|\beta$ -value difference|  $\geq 0.2$  were considered as being significantly differentially methylated loci. Limma is an R package that can provide an integrated solution for the data analysis of genomic experiments. It can not only handle complex experimental designs and test flexible hypotheses, but also make statistical conclusions more reliable when the numbers of samples are small [20]. For quality control, the CpG sites with missing values or detection *P* values  $> 0.05$  in  $> 95\%$  of articular cartilage specimens were eliminated.

### 2.5. Gene set enrichment analysis

Gene set enrichment analysis of differentially methylated loci were conducted by the Database for Annotation, Visualization and Integrated Discovery (DAVID) tool (<http://david.abcc.ncifcrf.gov/>) [21] and the GREAT tool (<http://great.stanford.edu/public/html/>) [22], respectively. DAVID has good power to make functional annotation of target gene sets, considering both gene ontology (GO) and biochemical pathways. Molecular function, cellular component and biologic process were considered for GO enrichment analysis. During the DAVID analysis, Fisher Exact test was adopted to measure the enrichment levels of target gene sets in annotation terms. A modified Fisher Exact *P* value was calculated by DAVID for each pathway [21]. GREAT is able to assign biologically meaning to a group of non-coding genomic regions by analyzing the annotations of the nearby genes. A hypergeometric test was implemented by GREAT to calculate the *P* value for each annotation term [22].

### 2.6. Mass spectrograph analysis

To validate the accuracy of genome-wide DNA methylation profiling, 12 CpGs loci of the significantly differentially methylated genes in genome-wide DNA methylation profiling were selected for further

**Table 2**  
List of the primers used for mass spectrograph analysis.

Name	Left primer	Right primer	Target length	Target CpG	CpG analyzed InT
cg04145890-1	GTTAGGGAGGTTTGGAGGTTTT	ACCCTTAAAAACAACCTTAATCCCA	253	11	9
cg07727358-1	TTTTTGAGTTAGGGTTGGGTAAGTT	CCAACCCCTACAAAATAAAAAATC	315	16	15
cg09911488-1	AATTTGTTTAGGATGTTGGGAGGT	AACTCAAAAAATTAACCTCACCCC	351	5	4
cg11849638-8	AGAAAGGAAGGGTAGGGTAAGTTTT	AACTCTATAAAACCCCACTAATCCC	247	5	3
cg12161489-3	TTGTTTTAGTTTTTGTAGTTGGG	TTTAAACAAAATTACTCCCTACCCC	267	5	5
cg16185996-2	GGTTTTAGTTAGGTTTTAGGGTTT	ATAATTTATTTTCCCTGCCAAAAAT	185	9	9
cg03717367	GTTTGGTTTTAAGGGGAATTTTTTA	TTCCCCTAACCTCTACTCTCTTAA	247	4	3
cg00779393	TTTTGGTAATATTGTGAGATTTTATGTTT	AATCTTACCTCTCAAATTTATTCGATCTA	499	3	3
cg04056837	GATTAAGGTAGTGTGTTGATTAAGGAGG	ATCTCCTCTAAAAACCCCTCCTAAC	499	2	2
cg08570033	GTGAGTGAATTTTTAGGAGATTTGA	AAACATAAACTCCTCATTACCTCAT	488	3	3
cg13172020	TGGTGTAGGAAAGTTAGAGAATATGTTG	AAACCTAACCAATCTAATACCCACC	375	5	5
cg18699025-14	TTTTTGTGGGGTAAGAGTTTG	TTTCCAAACCAACCAAAAAAC	318	15	15

mass spectrograph validation, including cg09911488, cg11849638 and cg12161489 in CARS gene, cg18699025, cg04145890, cg07727358 and cg16185996 in FGFR1 gene, cg04056837 of RUNX2 gene, cg08570033 and cg13172020 in PDE4D gene. Additionally, we also tested not statistically significant genes as a sensitivity test, including cg00779393 of RPF1 and cg03717367 of MAN1B1. Mass spectrograph analysis was conducted to validate the accuracy of genome-wide DNA methylation profile data using an independent hip articular cartilage sample from 10 ONFH patients and 10 healthy control subjects, matched for sex. QIAamp DNA Mini Kit (QIAGEN) was used to process the extracted DNA according to manufacturer's protocol. The methylation levels of CpG sites were detected by Sequenom MassARRAY DNA platform following standard protocol. Methprimer was used to design PCR primers (<http://epidesigner.com>) (Table 2). EpiTyper software (Sequenom, CA) was used to generate the methylation data of cartilage specimens. *t*-test was conducted to assess the significance of DNA methylation difference between ONFH cases and health controls.

**2.7. Immunohistochemical experiment**

IHC was conducted to identify the protein expression level of identified candidate genes with ONFH using the hip cartilage samples from 4 ONFH patients and 4 control subjects, which were same to above MS samples. Based on previous pathogenetic study results of ONFH as well as the biological function of identified differentially methylated genes, CARS, ADAMTS12, PDE4D, LRP5 and RUNX2 were selected for IHC experiment. Cartilage specimens were fixed by paraformaldehyde, rinsed with phosphate buffered saline (PBS), decalcified and embedded in paraffin. The paraffin-embedded hip articular cartilage tissues were sectioned (approximately 5–8 μm Thick), placed on glass slides, de-waxed in xylene, hydrated with graded ethanol, stained respectively by

hematoxylin and eosin (H&E), toluidine blue (TB) and Safranin O (SO) (Fig. 2). Then, the cartilage sections were treated with 3% hydrogen peroxide solution for 10 min, rinsed with PBS, and incubated with ADAMTS12, CARS, PDE4D, LRP5 and RUNX2 antibody at 4 °C overnight. The cartilage sections were then placed at 37 °C for 1 h, washed with PBS for 10 min, incubated with secondary antibody (Zhongshan Golden Bridge Biotechnology, China) at 37 °C for 15 min, exposed to Streptavidin-Horseradish Peroxidase (SHP) at 37 °C for 15 min, and stained with diaminobenzidine (DAB). We generated 5 cartilage sections from each cartilage specimen for each protein. For each cartilage specimen, the percentages of positive chondrocytes in 1000 chondrocytes were calculated separately from each of the 5 cartilage section for each protein. Finally, the mean percentage of positive chondrocytes of 5 cartilage sections was reported for each cartilage specimen. Because the pathological changes of hip cartilage varied from the superficial zone to deep zone in ONFH patients [7]. The superficial zone and deep zone of hip cartilage were scored separately for IHC. *t*-test was used to assess the significance of protein expression differences between ONFH patients and health controls at the superficial zone and deep zone of cartilage specimens, respectively. Differently expressed proteins were identified at *P* value < 0.008 after Bonferroni correction.

**3. Results**

**3.1. Differentially methylated loci in the articular cartilage of ONFH patients**

Fig. S1 shows the Pearson correlation analysis results of methylation β values of genome-wide DNA methylation profiles. Fig. S2 showed cutoff lines indicate the CpG sites with |β-value difference| ≥ 0.2 in Fig. S1. We detected 2872 differentially methylated CpGs sites between

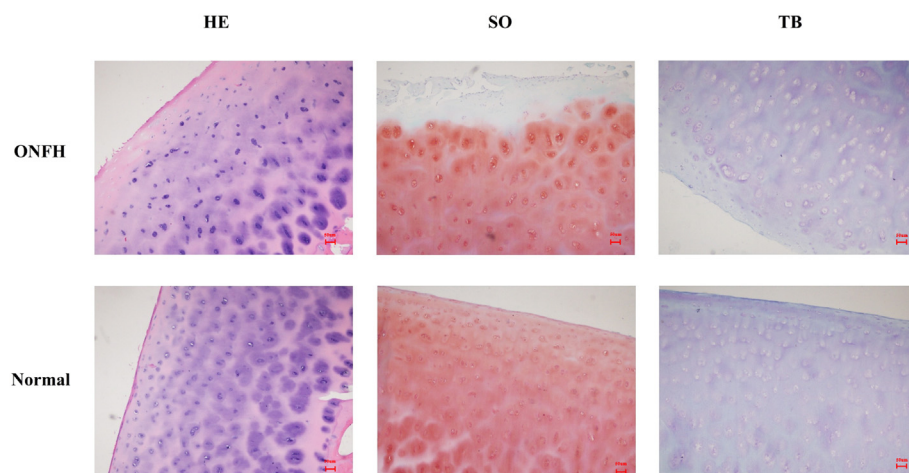


**Fig. 2.** Hematoxylin and eosin (HE), safranin O (SO) and toluidine blue (TB) staining of ONFH articular cartilage and normal articular cartilage. ONFH denotes necrosis of the femoral head. Normal denotes healthy controls. (For interpretation of the references to colour in this figure legend, the reader is referred to the web version of this article.)

**Table 3**  
List of top ten hypermethylated loci.

CpG	P-Value	Beta-difference	Gene name
cg10161198	$1.71 \times 10^{-6}$	0.37	FAM178B
cg03053125	$4.61 \times 10^{-6}$	0.23	
cg01904300	$5.31 \times 10^{-6}$	0.21	FAM178B
cg13990585	$1.09 \times 10^{-5}$	0.23	RGMA
cg15140902	$3.20 \times 10^{-5}$	0.21	FLJ22536
cg18699025	$5.00 \times 10^{-5}$	0.24	FGFRL1
cg26928799	$5.24 \times 10^{-5}$	0.20	
cg04956511	$5.38 \times 10^{-5}$	0.23	PTPN6
cg05255811	$5.44 \times 10^{-5}$	0.20	KCNK5
cg27447219	$6.33 \times 10^{-5}$	0.21	STK24

ONFH cases and normal controls, including 629 hypermethylated loci (corresponding to 480 hypermethylated genes, Table S1) and 2243 hypomethylated loci (corresponding to 1335 hypomethylated genes, Table S2), respectively. Table 3 showed top ten hypermethylated loci. Table 4 showed top ten hypomethylated loci. Across whole genome, the CpG locus cg09911488 ( $P$  value =  $2.28 \times 10^{-6}$ ,  $\beta$ -value difference =  $-0.2032$ ) within CARS gene was the most significant one for ONFH. We also identified several genes significantly differentially methylated between ONFH cases and healthy controls, such as FGFRL1 (cg18699025,  $P$  value =  $5.00 \times 10^{-5}$ ,  $\beta$ -value difference =  $0.2376$ ), ADAMTS12 (cg08160496,  $P$  value =  $8.78 \times 10^{-5}$ ,  $\beta$ -value difference =  $-0.2634$ ) and PDE4D (cg08570033,  $P$  value =  $1.82 \times 10^{-3}$ ,  $\beta$ -value difference =  $-0.3436$ ).

### 3.2. Mass spectrograph validation

The significantly differentially methylated genes in genome-wide DNA methylation profiling were selected for further mass spectrograph validation, including cg09911488, cg11849638 and cg12161489 in CARS gene, cg18699025, cg04145890, cg07727358 and cg16185996 in FGFRL1 gene, cg04056837 of RUNX2 gene, cg08570033 and cg13172020 in PDE4D gene. MS results showed that the cg12161489 ( $P$  value = 0.05) and cg11849638 ( $P$  value = 0.03) of CARS, cg04056837 ( $P$  value = 0.03) of RUNX2, cg08570033 ( $P$  value = 0.0008) and cg13172020 ( $P$  value = 0.005) of PDE4D gene presented significantly lower methylation level in ONFH cartilage as compared to normal cartilage. MS results found that cg18699025 ( $P$  value = 0.008) and cg16185996 ( $P$  value = 0.007), cg07727358 ( $P$  value = 0.01) and cg04145890 ( $P$  value = 0.02) of FGFRL1 gene presented higher methylation levels in ONFH cartilage as compared to normal cartilage. In addition, we also tested not statistically significant genes as a sensitivity test, including cg00779393 of RPF1 and cg03717367 of MAN1B1. We found that cg00779393 ( $P$  value = 0.36) and cg03717367 ( $P$  value = 0.17) were not significant in MS analysis. The results of MS validation were consistent with that of genome-wide DNA methylation profiling, confirming the accuracy of DNA methylation profiles data.

**Table 4**  
List of top ten hypomethylated loci.

CpG	P-Value	Beta-difference	Gene name
cg09911488	$2.28 \times 10^{-6}$	$-0.20$	CARS
cg26449334	$5.07 \times 10^{-6}$	$-0.22$	
cg21724915	$5.15 \times 10^{-6}$	$-0.32$	FTO
cg11849638	$1.36 \times 10^{-5}$	$-0.26$	CARS
cg03180359	$1.50 \times 10^{-5}$	$-0.26$	
cg09104383	$1.73 \times 10^{-5}$	$-0.35$	ARHGAP26
cg01886323	$2.68 \times 10^{-5}$	$-0.42$	
cg10925915	$3.65 \times 10^{-5}$	$-0.22$	
cg27052537	$3.85 \times 10^{-5}$	$-0.21$	
cg02207386	$3.92 \times 10^{-5}$	$-0.22$	

### 3.3. Gene set enrichment analysis

Table S3 summarizes DAVID GO enrichment analysis results. GO enrichment analysis identified 121 GO terms for biologic process, such as bone morphogenesis ( $P$  value =  $1.93 \times 10^{-4}$ ), chondrocyte differentiation ( $P$  value =  $8.17 \times 10^{-4}$ ), bone resorption ( $P$  value =  $2.34 \times 10^{-2}$ ), 49 GO terms for cellular component, such as golgi apparatus ( $P$  value =  $1.74 \times 10^{-3}$ ), cilium ( $P$  value =  $5.08 \times 10^{-3}$ ), semaphorin receptor complex ( $P$  value =  $5.59 \times 10^{-3}$ ), 43 GO terms for molecular function, such as semaphorin receptor activity ( $P$  value =  $6.73 \times 10^{-3}$ ), actin binding ( $P$  value =  $2.75 \times 10^{-2}$ ), ATP binding ( $P$  value =  $4.02 \times 10^{-2}$ ).

For pathway enrichment analysis, DAVID identified 9 biological pathways for hypermethylated genes, such as inflammatory mediator regulation of TRP channels signaling pathways ( $P$  value =  $1.16 \times 10^{-3}$ ), endocytosis signaling pathways ( $P$  value =  $1.27 \times 10^{-2}$ ), axon guidance signaling pathways ( $P$  value =  $1.88 \times 10^{-2}$ ) (Table S4). DAVID also identified 49 biological pathways for hypomethylated genes, such as MAPK signaling pathway ( $P$  value =  $2.15 \times 10^{-2}$ ), AMPK signaling pathway ( $P$  value =  $2.06 \times 10^{-2}$ ), PI3K-Akt signaling pathway ( $P$  value =  $4.90 \times 10^{-2}$ ), inflammatory mediator regulation of TRP channels signaling pathway ( $P$  value =  $1.45 \times 10^{-3}$ ) (Table S5).

GREAT detected 424 pathways (all  $P$  value < 0.05) for hypomethylated genes, such as MAPK signaling pathways ( $P$  value =  $9.78 \times 10^{-7}$ ), FGF signaling pathway ( $P$  value =  $6.26 \times 10^{-3}$ ), AP-1 transcription factor network ( $P$  value =  $5.93 \times 10^{-13}$ ), ECM-receptor interaction signaling pathway ( $P$  value =  $1.91 \times 10^{-7}$ ), TGF-beta receptor signaling pathway ( $P$  value =  $2.66 \times 10^{-6}$ ), p38 MAPK pathway ( $P$  value =  $2.05 \times 10^{-5}$ ) (Table S6).

### 3.4. Immunohistochemical analysis

Based on previous pathogenetic study results of ONFH and the biological function of identified differentially methylated genes, ADAMTS12 gene, CARS gene, PDE4D, gene, LRP5 gene and RUNX2 gene were selected for IHC experiments to explore their protein expression level with ONFH. As shown in Figs. 3 and 4, the protein expression levels of ADAMTS12, CARS, PDE4D, LRP5 and RUNX2 at the superficial zone and deep zone of ONFH cartilage specimens were significantly higher than that of control cartilage specimens (all  $P$  values < 0.05). IHC confirmed the increased protein expression of CARS (mean and 95%CI of superficial zone 59.67% [48.46, 56.14], and deep zone 31% [25.85, 30.61]), PDE4D (superficial zone 50.33% [33.64, 40.68] and deep zone 28.67% [10.81, 36.47]), ADAMTS12 (superficial zone 53.67% [36.01, 40.93] and deep zone 34.67% [22.56, 37.18]), LRP5 (superficial zone 59.63% [27.32, 39.61] and deep zone 22.95% [5.28, 19.29]), RUNX2 (superficial zone 52.58% [11.64, 31.33] and deep zone 35.01% [10.03, 27.44]) in ONFH articular cartilage. Figs. S3 and S4 showed the individual data points of IHC results.

## 4. Discussion

Recent studies have demonstrated the important roles of hip articular cartilage damage in the development of ONFH [1]. Clarifying the molecular mechanism underlying the destruction of ONFH articular cartilage may provide insight into the pathogenetic and therapeutic studies of ONFH. In this study, we conducted a genome-wide DNA methylation profiling of ONFH hip articular cartilage. Using independent validation samples, MS and IHC were further used to validate the accuracy of DNA methylation profiles data and protein expression level of candidate differentially methylated genes with ONFH hip articular cartilage damage. We observed significant DNA methylation alterations, and identified multiple candidate genes and pathways for ONFH hip articular cartilage damage. Our results suggest the implication of DNA

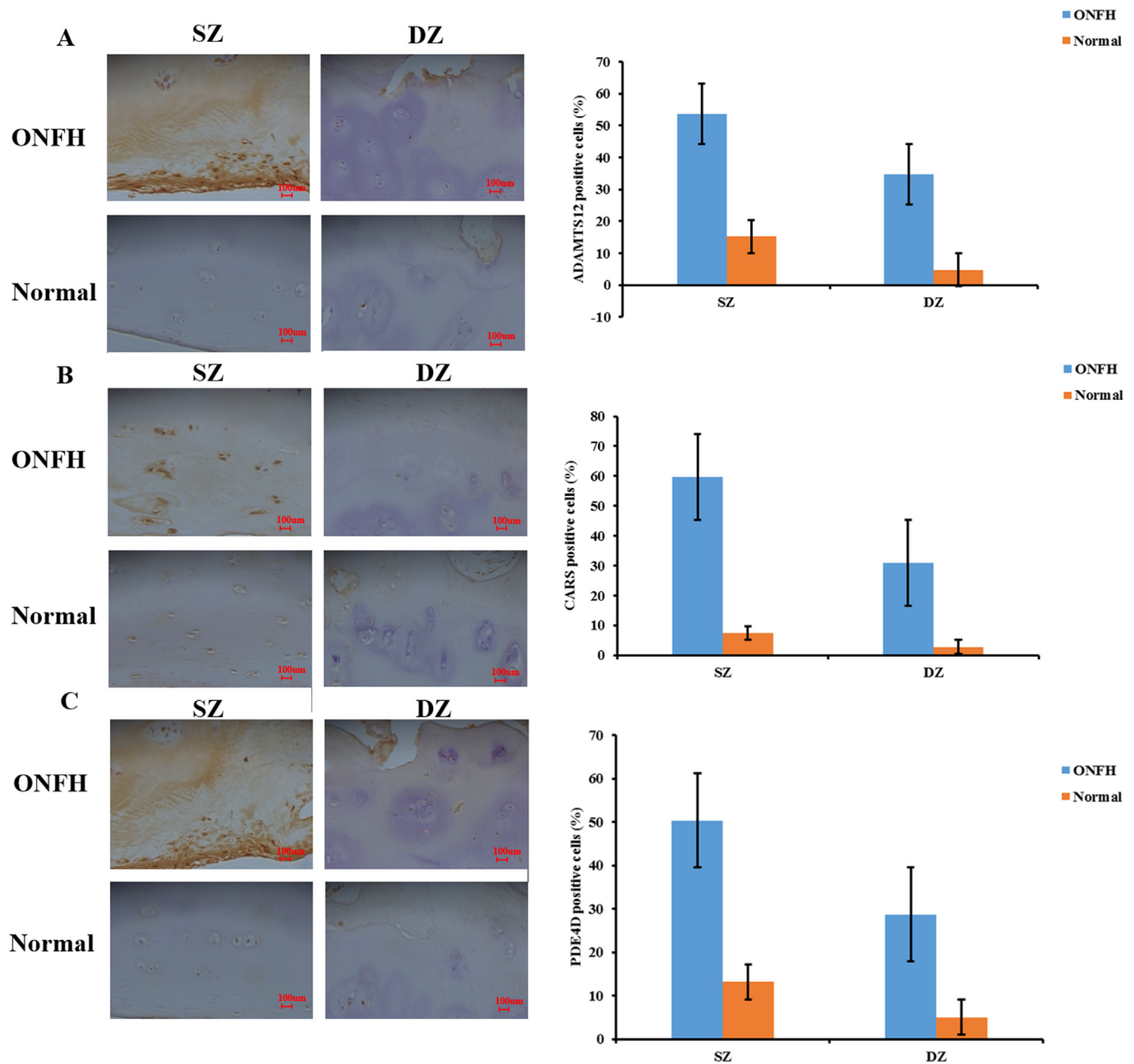


**Fig. 3.** Immunohistochemistry results for ADAMTS12 (A), CARS (B) and PDE4D (C) proteins in cartilage from patients with ONFH and normal hip cartilage. Original magnification  $\times 200$  of the superficial zone (SZ) and deep zone (DZ). \* $P$  value  $\leq 0.05$ , \*\* $P$  value  $\leq 0.001$ . ONFH means necrosis of the femoral head. The error bars represents the inter-individual variability of mean percentage of positive chondrocytes of CARS, ADAMTS12 and PDE4D proteins in immunohistochemical experiment.

methylation modification in the development of ONFH hip articular cartilage damage.

Cysteinyl-tRNA synthetase (CARS) encodes a class 1 aminoacyl-tRNA synthetase, which is involved in the regulation of mitochondrial biogenesis and bioenergetics [23]. Previous study found the important roles of mitochondrial function in the development of cartilage damage [24]. Mitochondrial dysfunction could result in excessive reactive oxygen species (ROS) production in pathological chondrocytes, as well as an increase in oxidative stress, deficiency of chondrocyte synthesis, inflammation and increased chondrocyte death [25]. Further studies are needed to explore the role of CARS in the mitochondrial dysfunction of ONFH cartilage. Additionally, CARS can synthesize cysteine polysulfides, which is associated with the initial translational process of de novo synthesis of nascent polypeptides in ribosomes. The functional studies of CARS are relatively limited by now. Akaike et al. found that

CARS played an important role in endogenous cysteine hydropersulfid (CysSSH) production [23]. Hayano M et al. found that loss of CARS could inhibit ferroptosis induced by cystine deprivation [26]. However, to the best of our knowledge, no effort has been paid to explore the possible role of CARS in the development of joint diseases, including ONFH. Further studies are needed to confirm our findings and clarify the potential mechanism of CARS involved in the development of ONFH.

We observed decreased DNA methylation status and increased protein expression levels for ADAMTS12 (a disintegrin and metalloprotease with thrombospondin domains) in ONFH hip articular cartilage. It has been demonstrated that ADAMTS enzymes are involved in the development of cartilage destruction, and play diverse roles in tissue morphogenesis, inflammation and vascular biology. For instance, Ji et al. observed that FGF2-mediated upregulation of Runx2 and

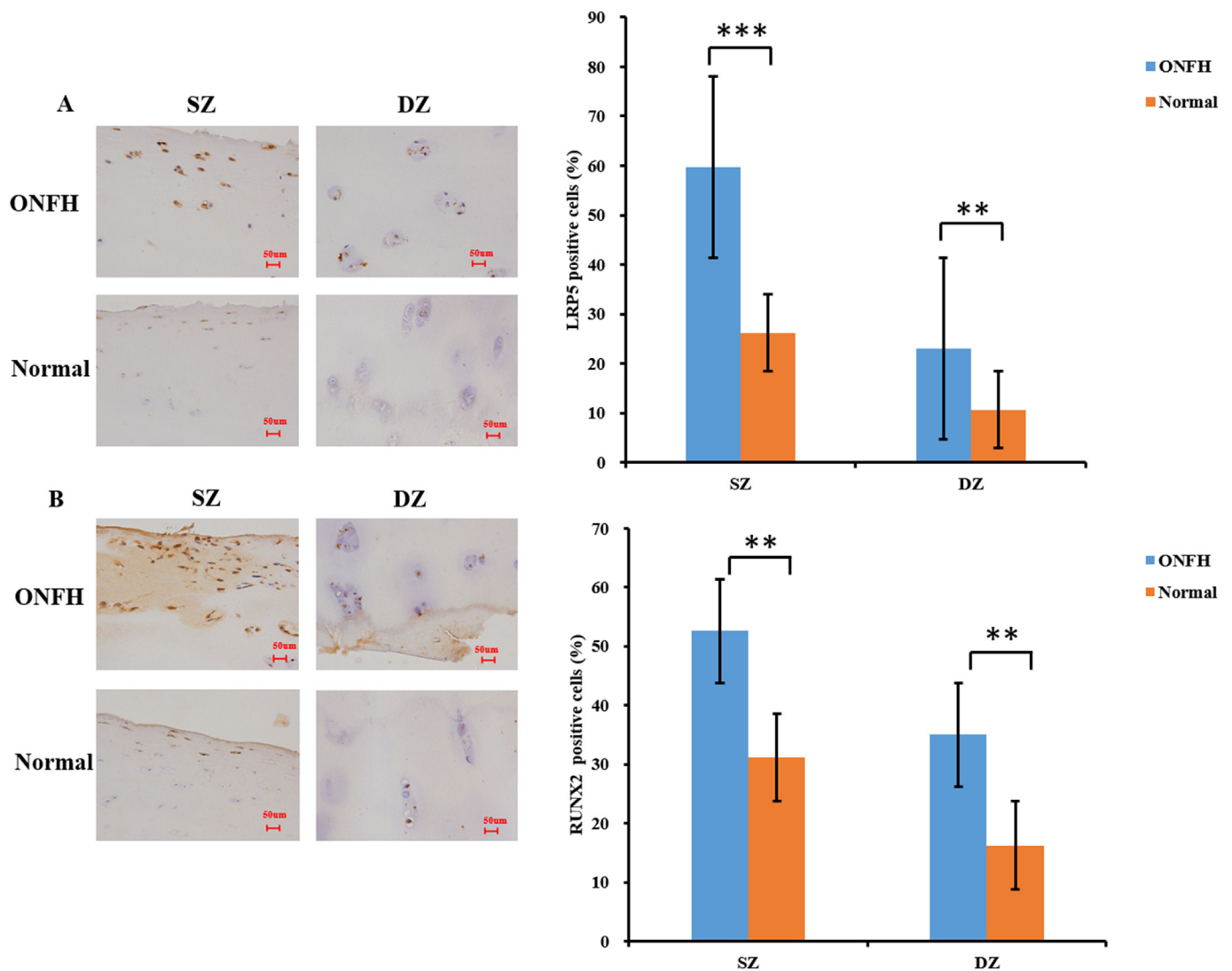


**Fig. 4.** Immunohistochemistry results for LRP5 (A), RUNX2 (B) proteins in cartilage from patients with ONFH and normal hip cartilage. Original magnification  $\times 200$  of the superficial zone (SZ) and deep zone (DZ). \* $P$  value  $\leq 0.05$ , \*\* $P$  value  $\leq 0.001$ . ONFH means necrosis of the femoral head. The error bars represents the inter-individual variability of mean percentage of positive chondrocytes of LRP5 and RUNX2 proteins in immunohistochemical experiment.

ADAMTS was involved in the pathogenesis of OA together with miR-105 [27]. Liu et al. suggested that the association between ADAMTS12 and COMP (cartilage oligomeric matrix protein) degradation played an important role in the development of arthritis [28]. Angela et al. found that ADAMTS12 was responsible for inflammatory response, and involved in neutrophil apoptosis, neovascularization and matrix remodeling in ADAMTS12 deficiency mice [29]. Wei et al. reported that deficiency of ADAMTS12 led to accelerated inflammatory arthritis in CIA mouse model [30]. Furthermore, previous studies have reported that inflammatory cytokines and cartilage destruction involved in the pathogenesis of ONFH [7,31]. Samara et al. observed that the genetic polymorphism of multiple inflammatory cytokine genes were significantly associated with the risk of osteonecrosis [32].

We also found that FGFR5 (fibroblast growth factor receptor like 1, also named FGFR5) was significantly differentially methylated between ONFH and healthy controls. FGFR5 is preferentially expressed in cartilage and bone [33]. FGFR5 can inhibit cell proliferation and promote cell differentiation. For example, Kahkonen et al. found that FGFR5 played critical roles in the differentiation of osteoblasts from mesenchymal stromal cell together with FGFR2 [34]. Another study also found an essential role of FGFR5 in the formation of cartilage elements [35]. Wilkie et al. found that the mutations of fibroblast

growth factor receptors (FGFRs) can cause chondrodysplasias [36]. Additionally, FGFR5 belongs to FGFR signaling pathway, which was also associated with ONFH in our pathway enrichment analysis. FGFR signaling pathway is involved in a diverse variety of biological processes, such as embryonic development, organogenesis, angiogenesis, wound healing and chondrocyte differentiation [37]. Extensive studies reported the important roles of FGFR signaling pathway in the development cartilage-associated diseases. For example, Silvie et al. reported that FGFR3 was associated with chondrocyte proliferation and chondrocyte extracellular matrix. FGFR3 signaling has effects on the regulation of MAP kinases, phospholipase C $\gamma$ , protein kinase B (PKB), Src, phosphatidylinositol 3-kinase, and AKT in cartilage [38]. Buchtova et al. found that the cooperation between aberrant FGFR signaling and WNT/ $\beta$ -catenin resulted in the suppression of chondrocyte differentiation [39]. Keiko et al. also found that FGFR signaling could activate WNT/ $\beta$ -catenin in chondrocytes [15].

We also identified several other candidate genes for ONFH, such as RUNX2, PDE4D and LRP5. RUNX2 (Runt-related transcription factor 2) is a transcription factor associated with osteoblastic differentiation and skeletal morphogenesis. Song et al. found that RUNX2 was associated with the risk of ONFH in Chinese population [40]. LRP5 (low-density lipoprotein receptor-related protein 5) is one of important genes

associated with bone remodeling. Jiang et al. found that LRP5 was implicated in the development of steroid-induced ONFH [41]. Interestingly, Aqueda et al. observed the functional relevance between RUNX2 and LRP5 [42]. PDE4D encodes Phosphodiesterase 4D protein, which plays an important role in degrading the second messenger cAMP. Yun et al. observed association between PDE4D and inflammatory activation in knock-in mice [43].

Both DAVID and GRRAT observed that mitogen-activated protein kinase signaling (MAPK) pathway was associated with ONFH in this study. MAPK is a mediator of matrix metalloproteinases in chondrocytes [44]. Multiple studies reported that MAPK pathway contributed to the development of chondrocytes and had positive effects on reducing cartilage resorption in arthritis. [45,46]. Adapala et al. reported that genes involved in MAPK pathway were significantly upregulated in ONFH, including growth factors (VEGF), inflammatory mediators (IL-6R) and several matrix related proteins FN1, TNC, COL6A1, ITGA5 and THBS3 [25]. Chen et al. found that 24 microRNAs were associated with GnRH signaling pathway and MAPK signaling pathway in pathogenesis of ONFH in buthionine sulphoximine (BSO) rat model by next-generation sequencing technology [42]. Wnt signaling is an important pathway, including the canonical pathway and the noncanonical pathway. Wnt signaling could regulate critical biological processes, such as cell differentiation and fate determination during embryogenesis and later stages of development [47]. Previous studies reported that Wnt activation was involved in cartilage homeostasis and degradation by stimulating matrix catabolic genes and activity in articular chondrocytes [48]. Zhang et al. found that Wnt signaling was associated with the pathogenesis of early stage steroid-induced ONFH (SANFH) by establishing a SANFH rat model [49]. Interestingly, previous studies observed functional interactions among MAPK, Wnt and FGF related pathways. For example, Buchtova et al. observed an interacting effect of FGF and WNT/ $\beta$ -catenin signaling pathways on the regulation of chondrocyte differentiation [39]. Chang et al. indicated that the interaction between Wnt-4 pathway and MAPK pathway had the potential to enhance bone regeneration [50].

There are three limitations that need to be noted in this study. First, the ages of ONFH case and control groups were not well matched in this study. ONFH usually affects the adults aged between 35 and 55. But normal cartilage specimens were collected from the patients with femoral neck fracture, which mostly occurred over 60 years. It is very difficult to collect normal hip cartilage specimens from the adults with ages < 55 years. To control the possible impact of age differences between ONFH and control samples, generalized linear mixed model has been used to adjust age as covariate during the DNA methylation profiles analysis. However, adjusting age as covariate may not completely eliminate the potential impact of age differences on our DNA methylation profile analysis. Second, the aim of this study is to scan candidate ONFH associated genes with altered DNA methylation levels in ONFH cartilage. We identified a group of differently methylated genes, which provided useful information for future pathogenetic studies of ONFH. Further biological studies, such as cell and animal experiments, are needed to explore the potential biological mechanism of identified candidate genes implicated in the development of ONFH. Third, the control sample specimens were collected from the patients with femoral neck fracture. The potential impact of femoral neck fracture on DNA methylations may affect the accuracy of our study results. Previous studies have observed the impact of non-genetic factors on DNA methylation levels. For example, Barres et al. found that high intensity exercise could result in reduced DNA methylation in skeletal muscle [15]. However, to the best of our knowledge, no study has been reported to evaluate the possible effect of traumatic events on the DNA methylation levels of articular cartilage. To control the possible impact of traumatic event on DNA methylation, all of the normal cartilage specimens were collected from the subjects within the 24 h of traumatic femoral neck fracture.

In conclusion, we conducted a genome-wide DNA methylation

profiling of ONFH and normal hip articular cartilage, and identified a set of candidate genes and pathways for ONFH. To the best of our knowledge, this is the first study to explore the roles of DNA methylation in the hip articular cartilage destruction of ONFH. Our results suggest the implication of DNA methylation alterations in the development of ONFH, and provide novel clues for pathogenetic and therapeutic studies of ONFH.

Supplementary data to this article can be found online at <https://doi.org/10.1016/j.bone.2019.06.021>.

## Declaration of Competing Interest

The authors declare no conflict of interest.

## Acknowledgments

We are grateful to the patients, orthopaedic surgeons and nurses at Second Affiliated Hospital of Health Science Center of Xi'an Jiaotong University for providing the clinical material. Thank you to Zengtie Zhang in the Pathology Department for guidance of processing the tissues.

## Formatting of funding sources

This study was supported by the National Natural Science Foundation of China (81772411, 81472925, 81673112), and the Fundamental Research Funds for the Central Universities.

## References

- [1] K.N. Malizos, et al., Osteonecrosis of the femoral head: etiology, imaging and treatment, *Eur. J. Radiol.* 63 (1) (2007) 16–28.
- [2] D.-W. Zhao, et al., Prevalence of nontraumatic osteonecrosis of the femoral head and its associated risk factors in the Chinese population: results from a nationally representative survey, *Chin. Med. J.* 128 (21) (2015) 2843–2850.
- [3] J.R. Lieberman, et al., Osteonecrosis of the hip: management in the 21st century, *Instr. Course Lect.* 52 (2003) 337–355.
- [4] Osteonecrosis of the femoral head – Diagnosis and management, *Precision Medicine* 2 (2015) e868.
- [5] Y. Assouline-Dayyan, et al., Pathogenesis and natural history of osteonecrosis, *Semin. Arthritis Rheum.* 32 (2) (2002) 94–124.
- [6] W. Fukushima, et al., Nationwide epidemiologic survey of idiopathic osteonecrosis of the femoral head, *Clin. Orthop. Relat. Res.* 468 (10) (2010) 2715–2724.
- [7] R. Xu, et al., Investigations of cartilage matrix degeneration in patients with early-stage femoral head necrosis, *Med. Sci. Monit.* 23 (2017) 5783–5792.
- [8] R.A. Magnussen, F. Guilak, T.P. Vail, Cartilage degeneration in post-collapse cases of osteonecrosis of the human femoral head: altered mechanical properties in tension, compression, and shear, *J. Orthop. Res.* 23 (3) (2005) 576–583.
- [9] G. Hadjigeorgiou, et al., Genetic association studies in osteonecrosis of the femoral head: mini review of the literature, *Skelet. Radiol.* 37 (1) (2008) 1–7.
- [10] Liu, Y.-F., et al., Type II collagen gene variants and inherited osteonecrosis of the femoral head. *N. Engl. J. Med.*, 2005. 352(22): p. 2294–2301.
- [11] C.G. Zalavras, et al., The 677C > T mutation of the methylene-tetra-hydrofolate reductase gene in the pathogenesis of osteonecrosis of the femoral head, *Haematologica* 87 (1) (2002) 111–112.
- [12] G.M. Hadjigeorgiou, et al., Paraoxonase 1 gene polymorphisms in patients with osteonecrosis of the femoral head with and without cerebral white matter lesions, *J. Orthop. Res.* 25 (8) (2007) 1087–1093.
- [13] R. Jaenisch, A. Bird, Epigenetic regulation of gene expression: how the genome integrates intrinsic and environmental signals, *Nat. Genet.* 33 (2003) 245–254.
- [14] M.D. Rushton, et al., Characterization of the cartilage DNA methylome in knee and hip osteoarthritis, *Arthritis & Rheumatology* 66 (9) (2014) 2450–2460.
- [15] W. Wang, et al., Genome-wide DNA methylation profiling of articular cartilage reveals significant epigenetic alterations in Kashin-Beck disease and osteoarthritis, *Osteoarthr. Cartil.* 25 (12) (2017) 2127–2133.
- [16] R.P. Ficat, Idiopathic bone necrosis of the femoral-head - early diagnosis and treatment, *Journal of Bone and Joint Surgery-British Volume* 67 (1) (1985) 3–9.
- [17] P. Du, W.A. Kibbe, S.M. Lin, lumi: a pipeline for processing Illumina microarray, *Bioinformatics* 24 (13) (2008) 1547–1548.
- [18] A.E. Teschendorff, et al., A beta-mixture quantile normalization method for correcting probe design bias in Illumina Infinium 450 k DNA methylation data, *Bioinformatics* 29 (2) (2013) 189–196.
- [19] Smyth, G.K., Limma: Linear models for microarray data. *Statistics for Biology and Health*, ed. R. Gentleman, et al. vol. 2005. 397–420.
- [20] M.E. Ritchie, et al., Limma powers differential expression analyses for RNA-seq and microarray studies, *Nucleic Acids Res.* 43 (7) (2015) e47.

- [21] G. Dennis Jr. et al., DAVID: database for annotation, visualization, and integrated discovery, *Genome Biol.* 4 (9) (2003) R60.
- [22] C.Y. McLean, et al., GREAT improves functional interpretation of cis-regulatory regions, *Nat. Biotechnol.* 28 (5) (2010) 495–501.
- [23] T. Akaike, et al., Cysteinyln-tRNA synthetase governs cysteine polysulfidation and mitochondrial bioenergetics, *Nat. Commun.* 8 (1) (2017) 1177.
- [24] F.J. Blanco, R. Ignacio, R.R. Cristina, The role of mitochondria in osteoarthritis, *Nat. Rev. Rheumatol.* 7 (3) (2011) 161.
- [25] P. López de Figueroa, et al., Autophagy activation and protection from mitochondrial dysfunction in human chondrocytes, *Arthritis & rheumatology* (Hoboken, N.J.) 67 (4) (2015) 966–976.
- [26] M. Hayano, et al., Loss of cysteinyl-tRNA synthetase (CARS) induces the transsulfuration pathway and inhibits ferroptosis induced by cystine deprivation, *Cell Death Differ.* 23 (2) (2016) 270–278.
- [27] Q.B. Ji, et al., miR-105/Runx2 axis mediates FGF2-induced ADAMTS expression in osteoarthritis cartilage, *Journal of Molecular Medicine-Jmm* 94 (6) (2016) 681–694.
- [28] C.J. Liu, et al., ADAMTS-12 associates with and degrades cartilage oligomeric matrix protein, *J. Biol. Chem.* 281 (23) (2006) 15800–15808.
- [29] A. Moncada-Pazos, et al., ADAMTS-12 metalloprotease is necessary for normal inflammatory response, *J. Biol. Chem.* 287 (47) (2012) 39554–39563.
- [30] Wei, J.-I., et al., ADAMTS-12 protects against inflammatory arthritis through interacting with and inactivating proinflammatory CTGF. *Arthritis & Rheumatology*. 0(ja).
- [31] B. Chen, Y. Liu, L. Cheng, IL-21 enhances the degradation of cartilage through the JAK-STAT signaling pathway during osteonecrosis of femoral head cartilage, *Inflammation* 41 (2) (2018) 595–605.
- [32] S. Samara, et al., Predictive role of cytokine gene polymorphisms for the development of femoral head osteonecrosis, *Dis. Markers* 33 (4) (2012) 215–221.
- [33] M. Wiedemann, B. Trueb, Characterization of a novel protein (FGFRL1) from human cartilage related to FGF receptors, *Genomics* 69 (2) (2000) 275–279.
- [34] T.E. Kahkonen, et al., Role of fibroblast growth factor receptors (FGFR) and FGFR like-1 (FGFRL1) in mesenchymal stromal cell differentiation to osteoblasts and adipocytes, *Mol. Cell. Endocrinol.* 461 (2018) 194–204.
- [35] R. Hanaoka, et al., Zebrafish *gcmB* is required for pharyngeal cartilage formation, *Mech. Dev.* 121 (10) (2004) 1235–1247.
- [36] A.O.M. Wilkie, Bad bones, absent smell, selfish testes: the pleiotropic consequences of human FGF receptor mutations, *Cytokine Growth Factor Rev.* 16 (2) (2005) 187–203.
- [37] B. Trueb, Biology of FGFRL1, the fifth fibroblast growth factor receptor, *Cell. Mol. Life Sci.* 68 (6) (2011) 951–964.
- [38] R. Liu, et al., Comparative analysis of gene expression profiles in normal hip human cartilage and cartilage from patients with necrosis of the femoral head, *Arthritis Res Ther* 18 (1) (2016) 98.
- [39] M. Buchtova, et al., Fibroblast growth factor and canonical WNT/beta-catenin signaling cooperate in suppression of chondrocyte differentiation in experimental models of FGFR signaling in cartilage, *Biochimica Et Biophysica Acta-Molecular Basis of Disease* 1852 (5) (2015) 839–850.
- [40] Y. Song, et al., Association of gene variants of transcription factors PPAR gamma, RUNX2, Osterix genes and COL2A1, IGFBP3 genes with the development of osteonecrosis of the femoral head in Chinese population, *Bone* 101 (2017) 104–112.
- [41] D.W. Zheng, et al., Differentially methylated regions in patients with rheumatic heart disease and secondary pulmonary arterial hypertension, *Experimental and Therapeutic Medicine* 14 (2) (2017) 1367–1372.
- [42] J. Chen, et al., Role of microRNAs in pathogenesis of osteonecrosis of the femoral head in BSO rat model, *Int. J. Clin. Exp. Pathol.* 9 (3) (2016) 3521–3528.
- [43] S. Yun, et al., Interaction Between Integrin alpha5 and PDE4D Regulates Endothelial Inflammatory Signalling, *vol. 18(10)*, (2016), pp. 1043–1053.
- [44] A. Liacini, et al., Inhibition of interleukin-1-stimulated MAP kinases, activating protein-1 (AP-1) and nuclear factor kappa B (NF-kappa B) transcription factors down-regulates matrix metalloproteinase gene expression in articular chondrocytes, *Matrix Biol.* 21 (3) (2002) 251–262.
- [45] V.Y. Tabakov, et al., Thiol antioxidants increase the intracellular level of reactive oxygen species and proliferation of SP2/0 mouse myeloma cells in serum-free medium, *Cell and Tissue Biology* 11 (2) (2017) 155–160.
- [46] G. Schett, et al., Activation, differential localization, and regulation of the stress-activated protein kinases, extracellular signal-regulated kinase, c-Jun N-terminal kinase, and p38 mitogen-activated protein kinase, in synovial tissue and cells in rheumatoid arthritis, *Arthritis Rheum.* 43 (11) (2000) 2501–2512.
- [47] N. Sassi, et al., The roles of canonical and non-canonical Wnt signaling in human differentiated articular chondrocytes, *Biotechnic & Histochemistry* 89 (1) (2014) 53–65.
- [48] T. Yuasa, et al., Wnt/beta-catenin signaling stimulates matrix catabolic genes and activity in articular chondrocytes: its possible role in joint degeneration, *Lab. Invest.* 88 (3) (2008) 264–274.
- [49] C. Zhang, et al., Apoptosis associated with Wnt/beta-catenin pathway leads to steroid-induced avascular necrosis of femoral head, *BMC Musculoskelet. Disord.* 16 (2015) 10.
- [50] J. Chang, et al., Noncanonical Wnt-4 signaling enhances bone regeneration of mesenchymal stem cells in craniofacial defects through activation of p38 MAPK, *J. Biol. Chem.* 282 (42) (2007) 30938–30948.